Available online at www.sciencedirect.com
SCIENCE DIRECT®
Journal of Electroanalytical Chemistry 552 (2003) 19–34
Journal of Electroanalytical Chemistry
www.elsevier.com/locate/jelechem

Electrochemical processes at gold | thiourea-containing aqueous acid solution interfaces

A.E. Bolzán *, R.C.V. Piatti, A.J. Arvia

Instituto de Investigaciones Fisicoquímicas Teóricas y Aplicadas (INIFTA) (UNLP, CONICET), Sucursal 4, Casilla de Correo 16, (1900) La Plata, Argentina

Received 8 October 2002; received in revised form 26 November 2002; accepted 31 December 2002

Abstract

The electrochemical behaviour of thiourea (TU) on gold in acid solutions is investigated in the range −0.2 to 1.7 V (versus standard hydrogen electrode) by conventional and triangularly potential modulated voltammetry, rest potential (E_{rest}) measurements, rotating disk and rotating ring-disk techniques. The value of E_{rest} is determined by an electrochemical reaction involving formamidine disulphide (FDS), adsorbed TU and soluble $[Au(TU)_2]^+$ species. For TU concentrations (c_{TU}) in the range $1 \leqslant c_{TU} \leqslant 50$ mM, E_{rest} decreases linearly with log c_{TU} with a slope of approximately −0.090 V decade^{-1}, while in the range $0.1 \leqslant c_{TU} \leqslant 0.25$ mM, it approaches −0.120 V decade^{-1}. Conventional and triangularly modulated voltammetry data indicate the quasi-reversible adsorption of TU occurring in the range $-0.2 \leqslant E \leqslant 0.1$ V, and the electro-oxidation of TU to FDS in the range $0.2 \leqslant E \leqslant 0.9$ V, occurring simultaneously with the electrodissolution of gold yielding soluble $[Au(TU)_2]^+$ species. Both the electro-oxidation of TU and the electrodissolution of gold are under mass transfer control influenced by adsorbate formation. Different adsorbates from TU are produced depending on the adsorption potential and time. The electro-oxidation of these adsorbates in the range 0.9–1.7 V yields sulphate, carbon dioxide and CN residues. Reaction products are consistent with previous STM and FTIRS data. Comparative electrochemical data from FDS- and sulphide-containing solutions are also presented. Reaction pathways in which the participation of different adsorbates is considered, are discussed.

Keywords: Gold; Thiourea; Adsorbates; Formamidine disulphide; Electro-oxidation; Dissolution

1. Introduction

In recent years, interest in the electrochemical processes at different metal | thiourea (TU)-containing aqueous solution interfaces has increased both for the understanding of fundamental aspects of electrochemical interfaces involving sulphur-containing molecules on single crystal metal surfaces [1,2] and for the determination of the properties of TU as an additive in different technological applications. At low concentrations, TU is used as an additive in the electrodeposition of metals such as copper from acid solutions [3], whereas, at high concentrations, it is considered as a possible leachant in hydrometallurgy for the recovery of gold and silver from minerals [4–10]. These applications are related to the complexing properties of TU for those metals [11–15]. In fact, for gold, a number of complexes involving the $[Au(TU)_2]^+$ cation, such as $[Au(TU)_2]Br$ [16], $[Au(TU)_2]Cl$ [17] and $[Au(TU)_2]_2SO_4$ [17], have been produced, isolated and identified by X-ray diffractometry.

Recently, it has been shown that the electro-oxidation of TU on gold in acid solutions takes place in the potential range of both gold immunity and gold corrosion [4], although the relative contributions of the TU and gold electro-oxidation reactions depend on both the TU concentration (c_{TU}) and the range of applied potential. However, although the overall electro-oxidation process has been studied by a number of conventional electrochemical techniques [4,8,18,19], the available kinetic data and conclusions on the reaction mechanism are not thoroughly consistent.

* Corresponding author. Fax: 54-221-4254642.
E-mail address: aebolzan@inifta.unlp.edu.ar (A.E. Bolzán).

0022-0728/03/$ - see front matter
doi:10.1016/S0022-0728(03)00020-2

The electrodissolution of gold has been studied in aqueous TU solutions containing either acid [18] or alkali [10]. For the latter, the reaction is partially hindered due to passivation of gold by elemental sulphur from the irreversible decomposition of TU. This reaction can be suppressed by the addition of sodium sulphite that increases the stability of TU in solution and simultaneously reduces the electrodissolution potential of gold by decreasing its apparent activation energy [10]. In acid, gold electrodissolution proceeds with 100% efficiency for $E < 0.3$ V (standard hydrogen electrode, SHE), while for $E > 0.3$ V the reaction is accompanied by TU electro-oxidation to formamidine disulphide (FDS) and byproducts, decreasing the efficiency of the reaction [18]. Soluble TU-gold complexes are also formed in aqueous TU solutions containing ferric ions as the oxidant [8]. In this case, the reaction occurs via intermediate ferrous gold(I) species and the formation of gold-TU complexes by oxidation of TU to FDS with ferric ions. The formation of a stable ferric sulphate complex in ferric sulphate-containing acid solutions contributes, under batch operating conditions, to the depletion of TU [20].

In situ FTIRS measurements [21] have shown that at potentials below 1.2 V (SHE), the electro-oxidation of TU on gold produces soluble $[Au(TU)_2]_2SO_4$ concomitantly with the electro-oxidation of TU to FDS. Once the electrode potential reaches the threshold potential related to the formation of the oxygen-containing layer on gold, carbon dioxide, sulphate ions and CN-containing species in solution are formed.

Most of the reported work has focused on gold | TU aqueous solution interfaces in the c_{TU} and potential ranges of gold dissolution, i.e. at relatively high concentrations of TU and low anodic overvoltages. Therefore, it is convenient to extend the study to low concentrations of TU and high positive potentials where the oxygen-containing layer on gold is formed. The results will demonstrate that the electrochemical processes that have been described for leaching conditions will also be observed at low concentrations of TU.

This work deals with the electrochemical processes at gold | TU-containing and gold | FDS-containing aqueous acid interfaces over the range of potentials related to the thermodynamic stability of water. Conclusions from the participation of TU electrosorption reactions are derived from data resulting from different electrochemical techniques, which can be contrasted with STM patterns of TU on gold (1 1 1) [2,22]. Likewise, conclusions about product formation and reactant disappearance that are reported in this work have been confirmed by in situ FTIRS data [21]. Results allowed us to distinguish different electroadsorption and electrochemical reactions of TU and FDS on gold in acid, as well as gold complex formation. Competitive electroadsorption processes involving TU and FDS adsorbates can be considered precursors of the appearance of gold complex ion formation in solution. Accordingly, a pathway for TU electro-oxidation on gold in acid and its role in the gold electrodissolution process can be advanced.

2. Experimental

First, the rest potential (E_{rest}) of gold in TU-containing 0.5 M sulphuric acid under either nitrogen or oxygen saturation was determined in the range $0.1 \leqslant c_{TU} \leqslant 50$ mM. Similar experiments were made in 0.09 mM $[Au(TU)_2]_2SO_4$ + TU-containing 0.5 M sulphuric acid under nitrogen saturation in order to set a constant concentration of gold-TU complexes in solution. The values of E_{rest} were stable for at least 30 min.

Voltammetric runs were made to determine the potential range of the different electrochemical processes. For this purpose, a conventional glass electrochemical cell with a working polycrystalline gold wire electrode (0.25 cm^2 geometric area, J. Matthey, spec pure), a large platinum sheet (2 cm^2 apparent area), as the counter electrode, and a mercurous sulphate electrode were utilised. The working electrode was polished mechanically with alumina and rinsed with Milli-Q water before each experiment. Its real surface area $A = 0.69$ cm^2, was determined from the voltammetric oxygen layer electroreduction charge [23]. For the detection of soluble reaction products and the determination of kinetic parameters related to diffusion controlled reactions, voltammetric runs using a rotating gold disk (RDE) and a rotating gold-disk/gold-ring electrode (RRDE) were also performed. The geometric area of both disk electrodes was $A = 0.12$ cm^2, and the RRDE collection efficiency $N = 0.24$. Both the lower (E_l) and the upper (E_u) potential limits were adjusted, attempting to separate the different electrochemical processes occurring during gold anodisation. Potential scan rates were varied in the range $0.005 \leqslant v \leqslant 0.50$ $V\,s^{-1}$, and working electrode rotation speeds in the range $0 \leqslant \omega \leqslant 7000$ rpm.

To investigate the early stages of TU/FDS redox couple formation, runs were made using triangularly modulated (TM) linear potential voltammetry. This technique [24] is useful for discovering fast surface electrochemical processes occurring in the ms range [24–27]. Briefly, it consists of a slow, either linear or triangular potential scan modulated with a relatively fast triangular potential signal of frequency (f) and small amplitude (A_m). The latter provides a sequence of fast potential scan voltammograms of the reacting system superimposed to the slow potential scan. The shape of the current/potential envelope and its dependence on f and A_m provide a way to find the optimal coupling between the modulating signal and the rate of the electrochemical reaction by adjusting f and A_m. For

the present work, A_m and f were set to 0.040 V, and in the range $0.1 \leqslant f \leqslant 3$ kHz, respectively.

The electrosorption of TU on gold was studied by first immersing the electrode in either 0.1 or 0.5 mM TU + 0.5 M sulphuric acid for an adsorption time $0 \leqslant t_{ad} \leqslant 900$ s and holding the electrode potential at E_{ad} in the range $0.05 \leqslant E_{ad} \leqslant 1.05$ V. Subsequently, the electrode, held at E_{ad}, was removed from the cell, rinsed with Milli-Q water, and immersed in 0.5 M sulphuric acid at $E = 0.05$ V. Following this, a voltammogram at $v = 0.05$ V s^{-1} from 0.05 to 1.65 V to electro-oxidise TU adsorbates, and backwards to 0.05 V was run.

As adsorbates from either FDS or sulphide species might be related to those produced from TU, voltammograms of gold in 1 mM FDS + 0.5 M sulphuric acid, and 1 mM sodium sulphide + 0.5 M sulphuric acid were also recorded.

Aqueous working solutions were prepared from TU (Fluka, puriss.), FDS dihydrochloride (ICN, 97%), sodium sulphide (Merck, p.a.), sulphuric acid (97% Merck, p.a.) and Milli-Q* water. Before and during each experiment freshly prepared solutions were kept under nitrogen saturation.

A conventional potentiostat and a waveform generator were used for voltammetry. RRDE experiments were made with a type BI-PAD Tacussel bipotentiostat. Runs were made at 298 K. Electrode potentials in the text are given on the SHE scale.

3. Results

3.1. Rest potentials

For gold in TU-containing 0.5 M sulphuric acid, irrespective of whether the solution is under either nitrogen or oxygen saturation, the value of E_{rest} decreases with log c_{TU} (Fig. 1). The E_{rest} versus log c_{TU} plot exhibits a reasonable straight line with a slope -0.09 V decade^{-1} in the range $1 \leqslant c_{TU} \leqslant 50$ mM, this slope being also observed in solutions containing 9×10^{-2} mM of $[Au(TU)_2]_2SO_4$, although for the latter the values of E_{rest} are shifted to more negative values. Otherwise, for $0.25 < c_{TU} < 1$ mM, the values of E_{rest} approach a straight line with a slope of -0.120 V decade^{-1}. The above description is valid for data from nitrogen and oxygen saturated solutions at constant c_{TU}, although values of E_{rest} from the latter are slightly more negative than those from the former solutions. These results are a first indication of a c_{TU} dependent potential-determining reaction.

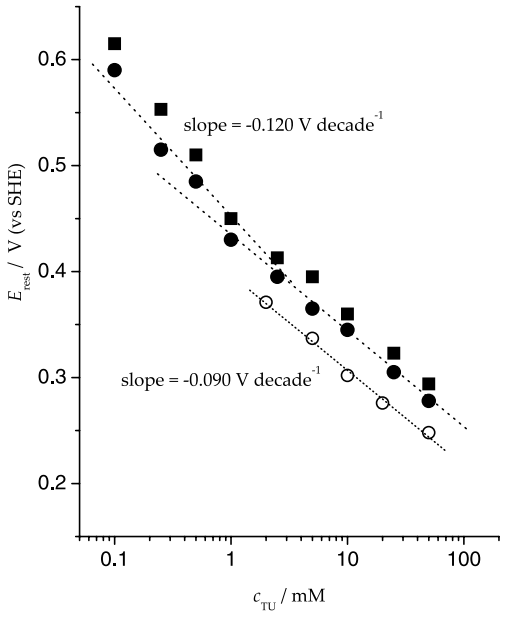

Fig. 1. Plots of E_{rest} versus c_{TU}. TU-containing aqueous 0.5 M sulphuric acid under nitrogen (■) and oxygen (●) saturation. (○) $c[Au(TU)_2]_2SO_4 = 9 \times 10^{-5}$ M under nitrogen saturation. 298 K.

3.2. TU-containing solutions

3.2.1. Voltammetric behaviour

Cyclic voltammograms of gold in 1 mM TU + 0.5 M sulphuric acid run at $v = 0.05$ V s^{-1} from $E_l = -0.05$ to $E_u = 1.6$ V show three anodic (Ia, IIa and IIIa) and two cathodic (Ic, IIIc) peaks (Fig. 2). For the sake of

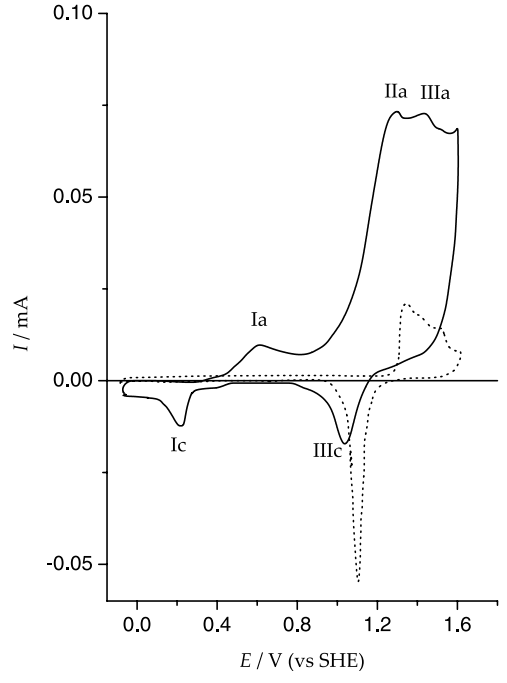

Fig. 2. Cyclic voltammogram of gold in 1 mM TU + 0.5 M sulphuric acid (full trace); gold in aqueous 0.5 M sulphuric acid (blank) voltammogram (dotted trace); $v = 0.05$ V s^{-1}. 298 K.

comparison a conventional voltammogram of gold in aqueous 0.5 M sulphuric acid is included in the figure. The pair of peaks Ia (0.62 V) and Ic (0.22 V) resembles that previously found for platinum [28] and copper [29]. This pair of peaks has been related to the TU/FDS redox system [30]. The anodic peak IIa at approximately 1.28 V is related to the electro-oxidation of gold as gold(I)–TU complex ions (hereafter denoted as gold complex ions) and the formation of byproducts from TU electro-oxidation [28]. Peak IIIa at 1.44 V can be associated with the formation of an oxygen-containing layer on gold from water electroadsorption yielding OH/O surface species [23,31,32]. The reverse scan shows peak IIIc at 1.05 V and a small cathodic hump that corresponds to the electroreduction of the oxygen-containing layer on gold. The small cathodic limiting current from 0.4 V downwards that overlaps peak Ic is related to the electroreduction of gold complex ions.

The voltammetry of the electrosorption of TU and the TU/FDS redox system on gold were investigated in the range of −0.2 to 0.9 V. Stabilised voltammograms run in the range between $E_l = 0.05$ and $E_u = 0.9$ V exhibit a single anodic peak Ia and two overlapping cathodic peaks Ic and IIc (Fig. 3a). The height of peaks Ia, Ic and IIc increases with v. The peak IIc/Ic height ratio increases with c_{TU} (Fig. 3b and c). On the other hand, when E_u is set at the potential of peak Ia, during the negative potential scan only peak Ic is observed (Fig. 3b and c, dashed trace), and simultaneously the cathodic current at the initial part of the reverse scan decreases (Fig. 3b and c). These results confirms that peak Ic is related to the electroreduction of FDS to TU, whereas peak IIc is related to the electroreduction of soluble gold complexes, their concentration increasing with both c_{TU} and E_u.

For $c_{TU} \leqslant 0.1$ mM, the height of peak Ia increases with $v^{1/2}$ approaching a single straight line plot (Fig. 4a). Conversely, for $c_{TU} > 0.1$ mM the plot shows two straight lines, one for $v < 0.05$ V s^{-1} and another for $v > 0.05$ V s^{-1} (Fig. 4a and b). The slope of these linear plots increases with c_{TU}, although in a way more complicated rather than that expected for a single electrochemical reaction under diffusion control [33]. The height of peak Ia is proportional to c_{TU} over the whole range of c_{TU} (Fig. 4c). Nevertheless, these plots also show that as v is increased, the straight line tends to exhibit a small positive ordinate at $v = 0$.

For those runs showing a single linear I_{pa} versus $v^{1/2}$ relationship, the voltammetric current peak is given by [33]

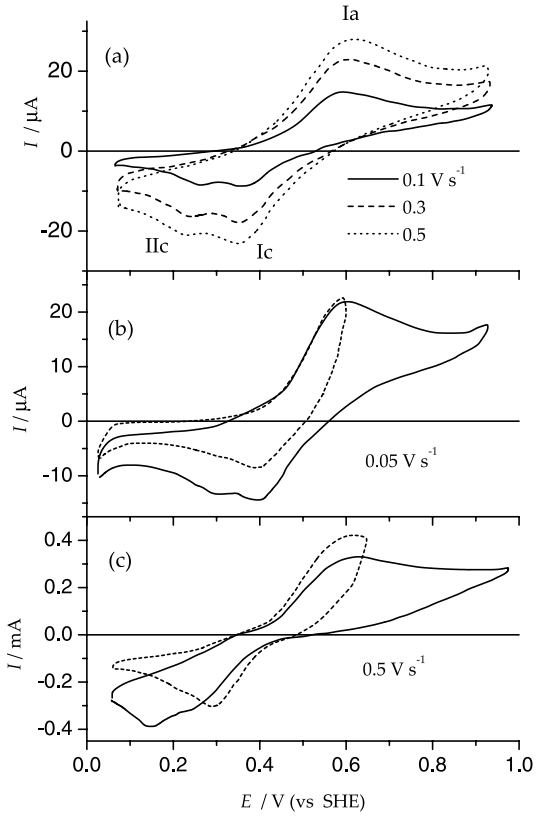

Fig. 3. (a) Cyclic voltammogram of gold between −0.2 and 0.9 V in: (a) 1 mM TU + aqueous 0.5 M sulphuric acid at different v values; (b) 1 mM TU + aqueous 0.5 M sulphuric acid at $v = 0.05$ V s^{-1}; (c) 10 mM TU + aqueous 0.5 M sulphuric acid at $v = 0.5$ V s^{-1}. 298 K.

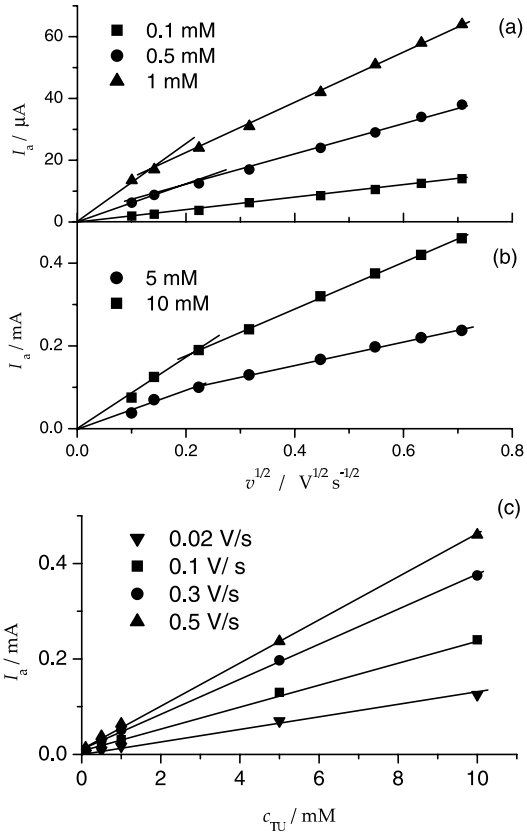

Fig. 4. (a and b) Plots of height of peak Ia versus $v^{1/2}$ for different c_{TU} values; (c) plot of the height Ia versus c_{TU} for different v values.

$$I_{pa} = 2.69 \times 10^5 n^{2/3} A D^{1/2} v^{1/2} c_{TU} \quad (1)$$

where n and D are the number of electrons and the diffusion coefficient of the reactant in the bulk of the solution, respectively, and A is the electrode area. Thus, taking the slope of $\Delta I_{pa}/\Delta v^{1/2} = 2 \times 10^{-5} A$ $V^{-1/2}$ $s^{1/2}$, $c_{TU} = 1 \times 10^{-7}$ mol cm^{-3}, $n = 1$, $A = 0.25$ cm^2, then it results in $D = 8.8 \times 10^{-6}$ cm^2 s^{-1}, a figure that agrees with the values of D for TU reported in Refs. [28,29,34,35].

The Gaussian deconvolution of peaks Ic and IIc for $c_{TU} = 1$ mM (Fig. 5a) shows that the charge density of peaks Ic (q_{Ic}) and IIc (q_{IIc}) decreases as v is increased, though the latter decreases rather faster than the former (Fig. 5b). Accordingly, the charge ratio q_{Ic}/q_{IIc} increases from approximately 0.5, for $v = 0.02$ V s^{-1}, to approximately 5 for $v = 0.5$ V s^{-1}, i.e. as v is increased, the contribution of peak Ic increases at the expense of peak IIc. These results indicate that as $v \to 0$ the yield of soluble gold complex electroformation tends to be greater than that from FDS electroreduction.

On the other hand, the potential of peaks Ic (E_{pI}) and IIc (E_{pII}) decreases almost linearly with log v with slopes

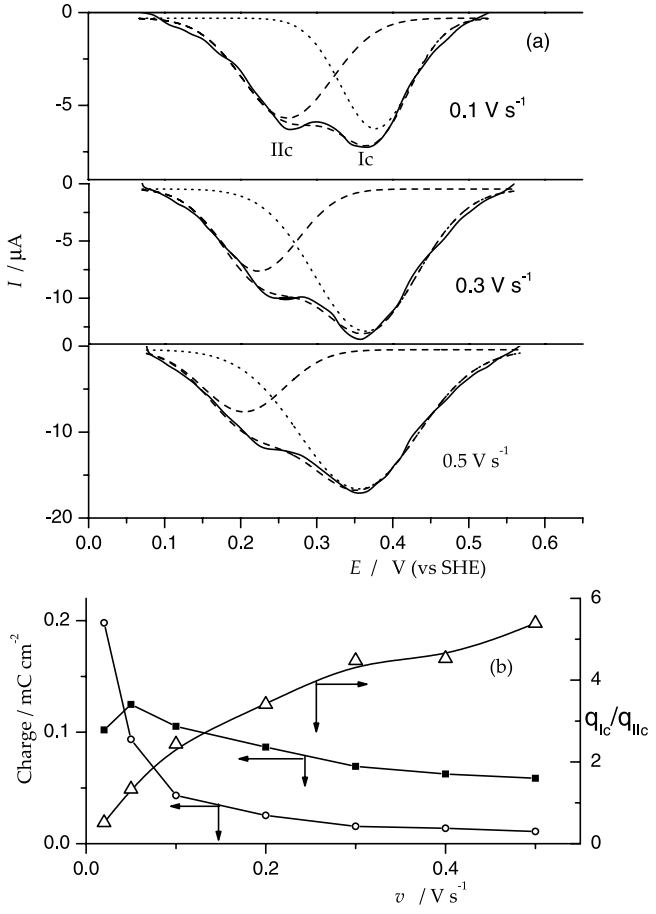

Fig. 5. (a) Deconvolution of peaks Ic and IIc from voltammograms run at different v values in 1 mM TU+aqueous 0.5 M sulphuric acid; (b) charge of peak Ic (■) and IIc (○) and their charge ration (△) versus v plot resulting from the deconvolution. 298 K.

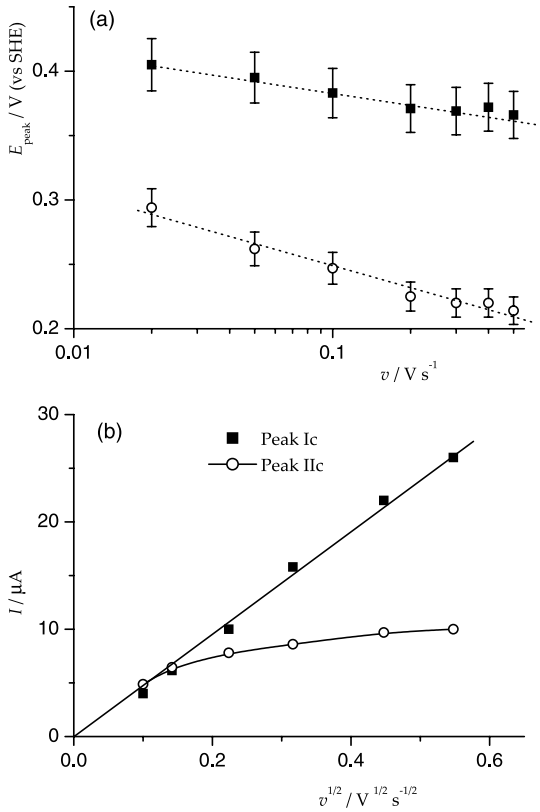

Fig. 6. Peak potentials versus v (a) and peak height versus $v^{1/2}$ (b) plots for peaks Ic and IIc resulting from deconvolution. 298 K.

of approximately 0.030 ± 0.005 and 0.060 ± 0.010 V decade^{-1}, respectively (Fig. 6a). Concomitantly, the difference $E_{pI} - E_{pII}$ increases with v. These results are consistent with a process under intermediate kinetics, i.e., a diffusion control reaction, its kinetics being influenced by the presence of adsorbates. Then, from the slopes of the linear E_p versus log v plots, the Tafel slopes (b_T) of processes associated with peaks Ic and IIc result in $b_T = -0.06$ and -0.120 V decade^{-1}, respectively.

The height of peak Ic increases linearly with $v^{1/2}$ while the height of peak IIc exhibits a linear increase with $v^{1/2}$ only at low v. For $v > 0.04$ V s^{-1}, this plot deviates from linearity tending asymptotically to a limiting value of $I_{pII} \simeq 10$ μA (Fig. 6b).

Conventional and modulated voltammetry experiments were also performed to investigate the behaviour of TU electrosorption on gold. Stabilised cyclic voltammograms of gold in 1 mM TU+0.5 M sulphuric acid run from $E_l = 0.05$ V to $E_u = 0.8$ V exhibit only peaks Ia and Ic (Fig. 7, full trace). However, as E_l is shifted from 0.05 to -0.2 V, the first negative potential scan shows a large contribution of peak IVc at approximately -0.1 V, and the subsequent reverse scan exhibits peak IVa at -0.05 V (Fig. 7, dotted line). The charge of these peaks decreases on cycling between -0.2 and 0.8 V, and simultaneously the height of peaks Ia and Ic decreases.

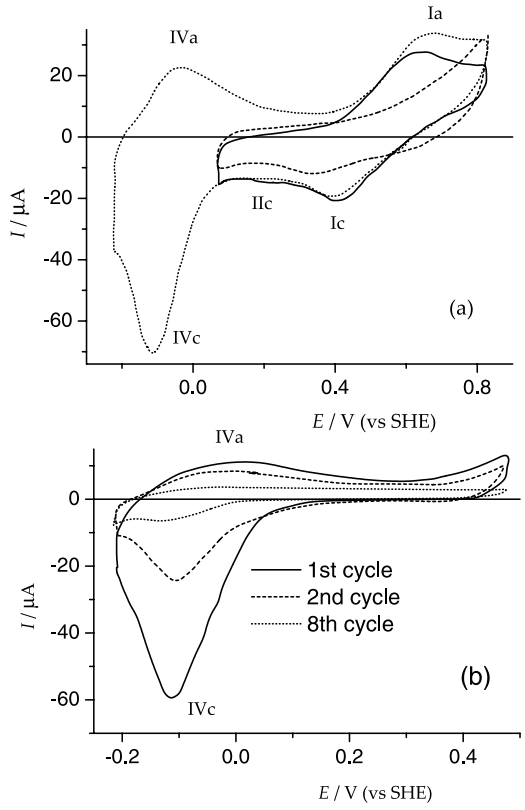

Fig. 7. (a) Voltammograms for gold run at $v = 0.05$ V s^{-1} in 0.5 mM TU+aqueous 0.5 M sulphuric acid resulting from the following conditions: (—) after 20 min cycling between $E_l = 0.15$ and $E_u = 0.8$ V; (- - -) first cycle after shifting E_l to -0.20 V; (. . .) first cycle after switching back E_l from -0.2 to 0.05 V; (b) voltammograms related to TU electosorption on gold run from E_{rest} downwards. 1 mM TU+ aqueous 0.5 M sulphuric acid. 298 K.

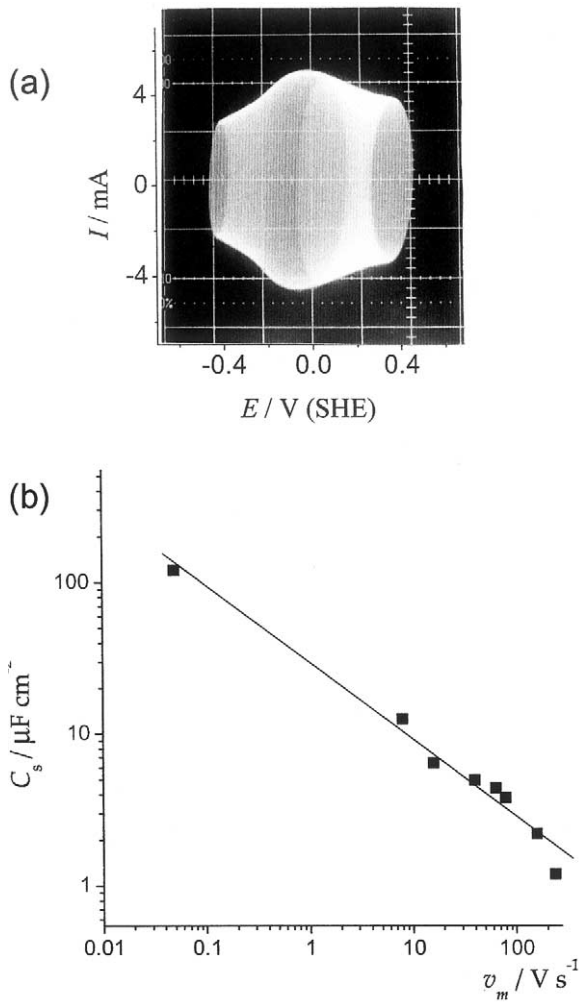

Fig. 8. (a) TM voltammogram of gold in 1 mM TU+aqueous 0.5 M sulphuric acid. $v = 0.5$ V s^{-1}, $f = 1$ kHz, $A_m = 0.04$ V. (b) Dependence of adsorbate pseudocapacitance on the modulating scan rate.

Eventually, when E_l is set back to 0.05 V, the charge of peaks Ia and Ic becomes considerably small and the potential of peak Ic shifts negatively (Fig. 7, dashed line).

Otherwise, the voltammograms of freshly polished gold in 1 mM TU+0.5 M sulphuric acid, started from $E = E_{rest}$ to -0.2 V (Fig. 7b), show peak IVc at approximately -0.1 V, the height of this peak decreasing with the number of cycles. The charge of peak IVc resulting from the first voltammogram is $q_{IIIc} \simeq 264$ μC cm^{-2} and decreases on cycling to attain an almost constant value $q_{IIIc} \simeq 30$ μC cm^{-2} after 8–10 cycles.

TM voltammograms of gold in 1 mM TU+0.5 M sulphuric acid in the potential range of peaks IVa/IVc, run at 0.5 V s^{-1}, $A_m = 0.040$ V and $f = 1$ kHz, display a voltammetric envelope with a capacitance contribution of 50 μF cm^{-2} at $E_l = -0.6$ V, 80 μF cm^{-2} at $E_u = 0.2$ V, and a pair of almost mirror image conjugated current peaks (Fig. 8a). The charge of these peaks is symmetrically distributed with respect to the null baseline current. This voltammogram provides a clear indication of a fast redox surface reaction at approximately -0.2 V.

Seemingly, the pair of peaks IVa/IVc (Fig. 7a) involves the fast electrodesorption of adsorbates that were accumulated on gold either spontaneously under open circuit conditions, or by potential cycling in the range of the TU/FDS redox couple. The electrodesorption of those adsorbates, which is accompanied by the discharge of hydrogen ions, results in a partial inhibition of TU electro-oxidation, probably caused by residual sulphur-species formed in the -0.2 to 0 V range.

TM voltammograms were also run at 0.05 V s^{-1}, $A_m = 0.040$ V and $0.1 \leqslant f \leqslant 3$ kHz. Thus, for constant f, the voltammograms exhibit a slight potential shift between the anodic and cathodic peaks and a symmetric distribution of the corresponding charges. From the modulated current peaks, the pseudocapacitance was determined as $C_s = I_p/v_m$, where I_p is the height of the current peak and $v_m = 2fA_m$, is the scan rate of the modulating signal. The log C_s versus log v_m plot (Fig. 8b) shows a single straight line with a slope -0.5, which extrapolates to the value of C_s for $v_m = 0.05$ V s^{-1}. This

indicates that the fast electrosorption process is mass transfer-controlled, in agreement with data obtained from conventional voltammetry.

3.2.2. Voltammetric electro-oxidation of TU adsorbates

The electro-oxidation of TU adsorbates was studied by first immersing the electrode in TU-containing 0.5 M sulphuric acid ($0.1 \leqslant c_{TU} \leqslant 0.5$ mM) at a preset potential ($0.05 \leqslant E_{ad} \leqslant 1.05$ V) for the time t_{ad} ($0 \leqslant t_{ad} \leqslant 900$ s). After holding the electrode at E_{ad} for t_{ad}, it was transferred to a second cell containing 0.5 M sulphuric acid. Subsequently, the voltammogram run from E_{ad} to 1.65 V and downwards to 0.05 V (Fig. 9a) shows a peak at approximately 1.25 V and a broad anodic contribution from 1.3 to 1.7 V. On increasing E_{ad} from 0.25 to 0.90 V, for $t_{ad} = 900$ s, both the peak at 1.25 V and the current contribution from 1.50 to 1.65 V increase, though the latter is less significant. However, once E_{ad} is set at 1.05 V for $t_{ad} = 900$ s, the peak at 1.25 V either disappears or shifts positively turning into a hump at approximately 1.30 V, and a peak at approximately 1.45 V. The adsorbate electro-oxidation charge density (q_{ad}), after correction for the charge related to the formation of the oxygen-containing layer on gold, results in $q_{ad} \simeq 630 \pm 0.02$ μC cm^{-2}, irrespective of E_{ad}.

Alternatively, for $E_{ad} = 1.05$ V and $15 \leqslant t_{ad} \leqslant 900$ s (Fig. 9b), the electro-oxidation voltammogram shows

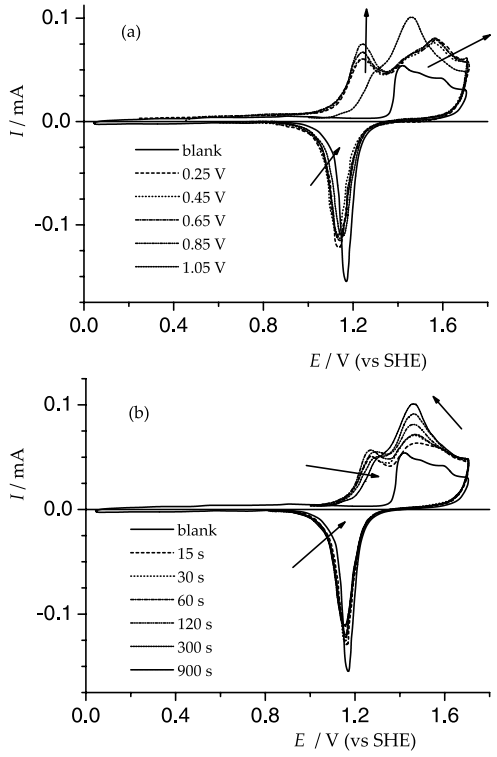

Fig. 9. Voltammograms of TU adsorbate electro-oxidation on gold. (a) $t_{ad} = 900$ s and different t_{ad} values; (b) $E_{ad} = 1.05$ V and different E_{ad} values. 0.1 mM TU+aqueous 0.5 M sulphuric acid. $v = 0.05$ V s^{-1}. 298 K.

peaks at approximately 1.25 and 1.45 V. The former tends to decrease and shifts positively as t_{ad} is increased, whereas the latter exhibits no potential shift, but increases with t_{ad}. In this case, q_{ad} increases from approximately 390 μC cm^{-2} to approximately 600 μC cm^{-2} as t_{ad} is changed from 15 to 900 s.

These results show that TU adsorbates are electro-oxidised in a two-stage process, the first stage occurring from 1.1 to 1.3 V (process I), and the second from 1.3 upwards (process II). Process I prevails for $E_{ad} < 1.0$ V or $t_{ad} < 300$ s, whereas process II prevails for $E_{ad} > 1.0$ V or $t_{ad} > 300$ s. For $c_{TU} = 0.1$ mM, the electro-oxidation charge depends neither on t_{ad} nor on E_{ad}. This means that as fast TU adsorption on gold proceeds, strongly bound residues are, at least in part, also formed. This conclusion agrees with differential capacity values that have previously been reported [36], showing a maximum coverage by TU on gold for $c_{TU} = 1.4$ μM [36]. The weak dependence of q_{ad} on t_{ad} (q_{ad} increases only approximately 50% for a 60-fold increase in t_{ad}) suggests that the increase in t_{ad} probably changes the nature of the adsorbates rather than increasing their surface concentration. Therefore, the first adsorbate electro-oxidation peak (process I) coincides with peak IIa and can be assigned to the electrodesorption of TU/FDS as gold complex. The second one (process II) occurs simultaneously with the formation of the oxygen-containing layer on gold. The current contribution of process II involves the electro-oxidation of TU residues.

3.2.3. RDE and RRDE voltammetry

For the electrochemical detection of soluble species RDE and RRDE voltammetry experiments were performed. The voltammetric behaviour of gold in x mM TU+0.5 M sulphuric acid ($0.1 \leqslant x \leqslant 50$), at $v = 0.005$ V s^{-1}, in the range $0.15 \leqslant E \leqslant 1.65$ V under rotation ($500 \leqslant \omega \leqslant 7000$ rpm) (Fig. 10), exhibits anodic peak Ia and a hump at approximately 0.95 V followed by peaks IIa and IIIa, already described in Section 3.2.1. The reverse scan shows a reactivation of the anodic process related to peak IIa. On increasing c_{TU}, the heights of all anodic peaks and humps increase, and their peak potentials shift negatively and a new small peak Va at 0.5 V begins to be observed. The possible origin of this peak could be inferred from RRDE data.

On the other hand, when the potential scan is reversed at 0.9 V, i.e. at the ascending branch of peak IIa (Fig. 10, inset), the anodic current exhibits a hysteresis loop that is consistent with the electrodissolution of gold via a gold surface complex.

For $c_{TU} \geqslant 5$ mM (Fig. 11f), single straight line plots of the height of peaks IIa and IIIa versus $\omega^{\frac{1}{2}}$ going through the origin of coordinates are obtained. This behaviour indicates that the corresponding reactions are under mass transfer control, in agreement with results reported

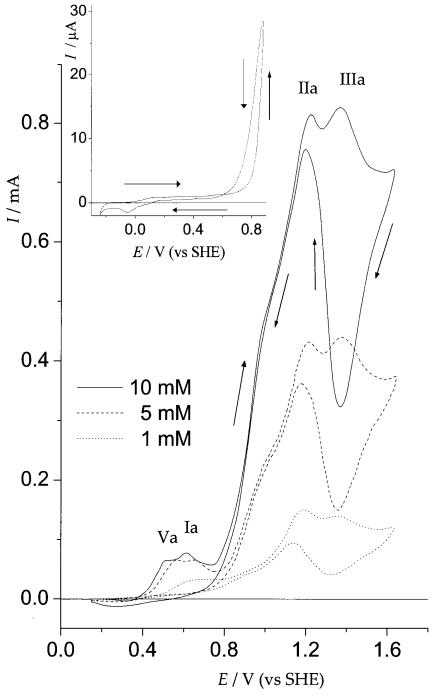

Fig. 10. RDE voltammograms run at 0.005 V s^{-1} at different c_{TU} values and $\omega = 2000$ rpm. The hysteresis loop resulting from potential scanning between $E_l = 0.15$ V and $E_u = 0.87$ V is shown ($x = 1$, inset). x mM TU + aqueous 0.5 M sulphuric acid. (···) $x = 1$; (---), $x = 5$; (—) $x = 10$. $A = 0.12$ cm^2.

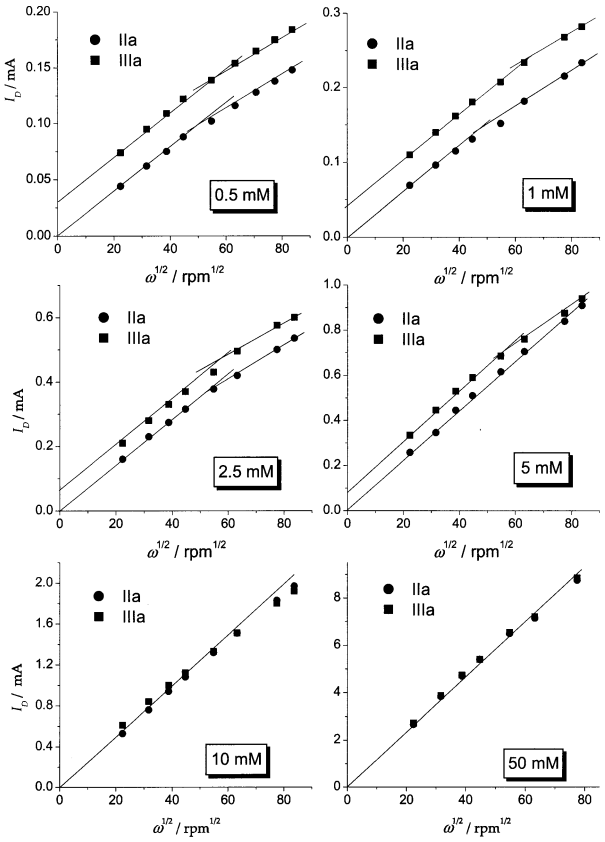

Fig. 11. Height of current peak from gold RDE voltammograms versus $\omega^{1/2}$ plots at different c_{TU}. 298 K.

above. At lower c_{TU}, the height of peak IIa versus c_{TU} plots show two straight line portions (Fig. 11a–d), the first one going through the origin of coordinates. The crossover appears practically for the same value of $\omega^{\frac{1}{2}}$, but for $I = I_D$ increases almost linearly with c_{TU}. This description can be extended to peak IIIa for $c_{TU} \leqslant 5$ mM, although in this case the straight line always presents a finite ordinate.

The fact that the finite current at $\omega = 0$ increases as c_{TU} is decreased confirms that at least two electrooxidation processes are competing in the potential range of peaks IIa and IIIa. This agrees with the fact that for constant ω, the height of peaks IIa and IIIa increases linearly with c_{TU}. The decrease in the slope $\Delta I_D/\Delta\omega^{\frac{1}{2}}$ for $\omega^{\frac{1}{2}} > 50$ that is observed as c_{TU} decreases (Fig. 11), indicates that the accumulation of residues at the electrode surface decreases the yield of the electrooxidation processes. Presumably, this effect might be due to the removal of surface species inhibiting the reactions related to peaks IIa and IIIa.

The formation of soluble anodic products was also detected with the RRDE at $\omega = 2000$ rpm under a linear potential scan at $v = 0.001$ V s^{-1} from 0.2 to 1.65 V, setting the potential of the ring at $E_R = 0.2$ V. Under these conditions, soluble species that are formed at the disk in the range 0.4 to 1.65 V are caught and electroreduced at the ring (Fig. 12). Potential scans

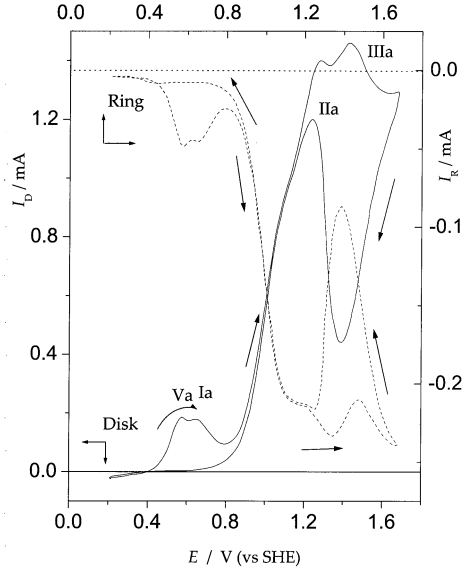

Fig. 12. Ring (dotted line) and disk gold electrode (full trace) current versus potential plots run at 0.01 V s^{-1}; $\omega = 2000$ rpm; $E_R = 0.2$ V. Arrows indicate the direction of the potential scan. 1 mM TU + aqueous 0.5 M sulphuric acid. 298 K.

display a current at the ring that looks like the mirror image of the current at the disk. Thus, for $E > 0.4$ V, the cathodic current at the ring increases with the anodic

current at the disk. A pair of cathodic peaks at 0.56 and 0.66 V, simultaneously with anodic peaks Va and Ia at the disk, are observed. Then, the cathodic current at the ring reaches a plateau at 1.15 V and increases in the potential range 1.50 to 1.65 V. On the reverse scan, I_R decreases to a minimum at $E_D \simeq 1.40$ V, and later increases to reach a current plateau at 1.15 V, and eventually decreases to zero. In the range 0.4 to 0.8 V, the current ratio results in $I_R/I_D \simeq 0.25$, in agreement with the collection efficiency of the RRDE. This figure indicates the complete electroreduction of soluble products, either FDS or gold complex ions that were formed during the anodisation in the potential range 0.2–1.65 V. For $E > 0.8$ V, I_R/I_D decreases to 0.17, a figure that indicates a decrease in the yield of the electroreduction reactions at the ring electrode due to the formation of products that partially passivate the disk electrode surface [21].

3.3. FDS-containing solutions

3.3.1. Stabilised cyclic voltammograms

In our work, the voltammetric response of FDS on gold occurs in the presence of hydrochloric acid. Accordingly, the voltammetric features of FDS on gold should be influenced by competitive adsorption of TU, FDS, water and chloride ions. The cyclic voltammogram of gold in 1 mM FDS+2 mM hydrochloric acid+0.5 M sulphuric acid, run at $v = 0.05$ V s^{-1} between −0.05 and 1.7 V (Fig. 13a), exhibits the pair of peaks I′a/I′c due to the TU/FDS redox system, the pair of peaks (II′a+VI′a)/peak VI′c related to the electrodissolution of gold as Au(I) and Au(III) chloride complexes [37], and the pair of peaks III′a/III′c associated with the oxygen-containing layer redox system. FDS voltammetric peaks are denoted with roman primes.

The change of E_u stepwise from 1.20 to 1.45 V increases the height of peak VI′c, but for $E_u > 1.45$ V peak III′c emerges (Fig. 13b) at the expense of peak VI′c. It is known [37] that the electrodissolution of gold in chloride-containing acid in the range 1.0 to approximately 1.5 V is accompanied by the partial coverage of gold with an oxygen-containing layer.

When the potential window is limited to the range 0.05–0.85 V (Fig. 14a) only the pair of peaks I′a/I′c, both preceded by ill-defined humps, can be seen. For $v^{1/2} \leqslant 0.4$ V$^{1/2}$ s$^{-1/2}$ the height of peaks Ia and Ic, after baseline correction, increases linearly with $v^{1/2}$ (Fig. 14b) and the linear plot intersects the origin of coordinates, as expected for a conjugated electrochemical process under diffusion control [33]. For $v^{1/2} \geqslant 0.4$ V$^{1/2}$ s$^{-1/2}$, the plot corresponding to peak Ic exhibts a second straight line portion with a lower slope. This behaviour is consistent with that depicted in Fig. 4.

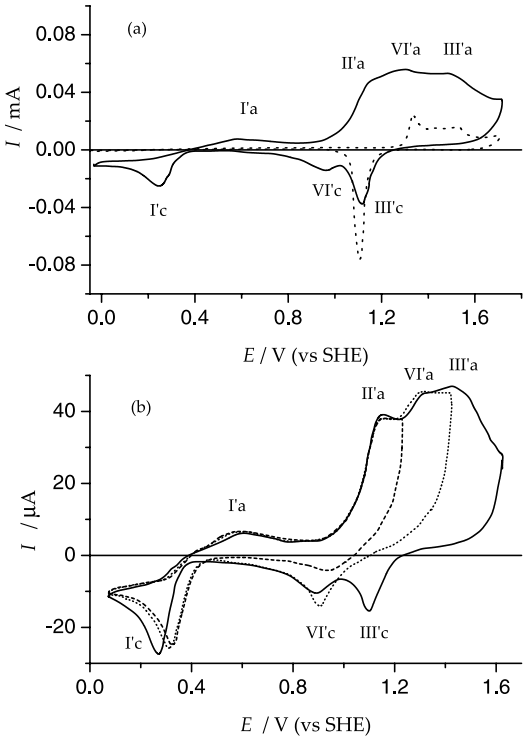

Fig. 13. (a) Cyclic voltammogram of gold in 1 mM FDS (2 mM HCl)+aqueous 0.5M sulphuric acid (full trace); blank voltammogram (dotted line). (b) Stepwise increase of E_u form 1.2 to 1.6 V s^{-1}. $v = 0.05$ V s^{-1}.

When E_l is shifted from 0.05 to −0.2 V (Fig. 14c), the voltammogram shows a small cathodic peak IV′c at approximately −0.07 V related to TU electrodesorption similar to that observed for TU-containing solutions (Fig. 7), although the decrease in height of this peak during cycling is less significant than for TU.

3.3.2. RDE voltammograms

RDE voltammograms of gold in FDS-containing solutions run from −0.1 to 1.7 V at $v = 0.05$ V s^{-1} and $\omega = 2000$ rpm (Fig. 15a) show a single somewhat asymmetric broad anodic peak at approximately 1.4 V, covering the potential range 1.0–1.6 V, i.e., where peaks II′a, VI′a and III′a are seen. The reverse scan exhibits peak III′c at approximately 1.1 V, and a limiting current that extends from approximately 0.3 V downwards. The comparison of the voltammogram depicted in Fig. 15a with that obtained in quiescent solutions (Fig. 13) shows that stirring causes the disappearance of peak VI′c (Fig. 15a) and that peak I′c, assigned to the electroreduction of FDS, turns into a cathodic limiting current ($I_{c,l}$) (Fig. 15). This was confirmed by setting $E_u = 0.85$ V, i.e. where gold electrodissolution, due to the presence of chloride ions, does not occur [37], and changing the concentration of FDS. In both cases, the linear dependence of the cathodic limiting current on $\omega^{1/2}$ is verified (Fig. 15b). Accordingly, as a first approximation, let us

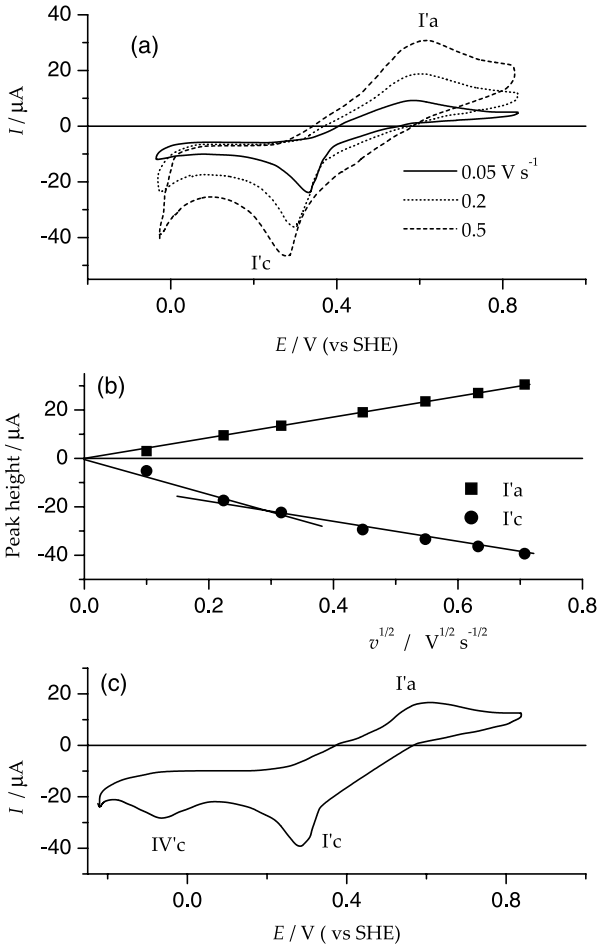

Fig. 14. (a) Cyclic voltammogram of gold in 1 mM FDS (2 mM HCl)+aqueous 0.5 M sulphuric acid at different v values. (b) Dependence of the height of peaks I′a and I′c on the square root of v. (c) Cyclic voltammogram recorded after changing E_λ from 0.05 to −0.2 V; $v = 0.05$ V s^{-1}.

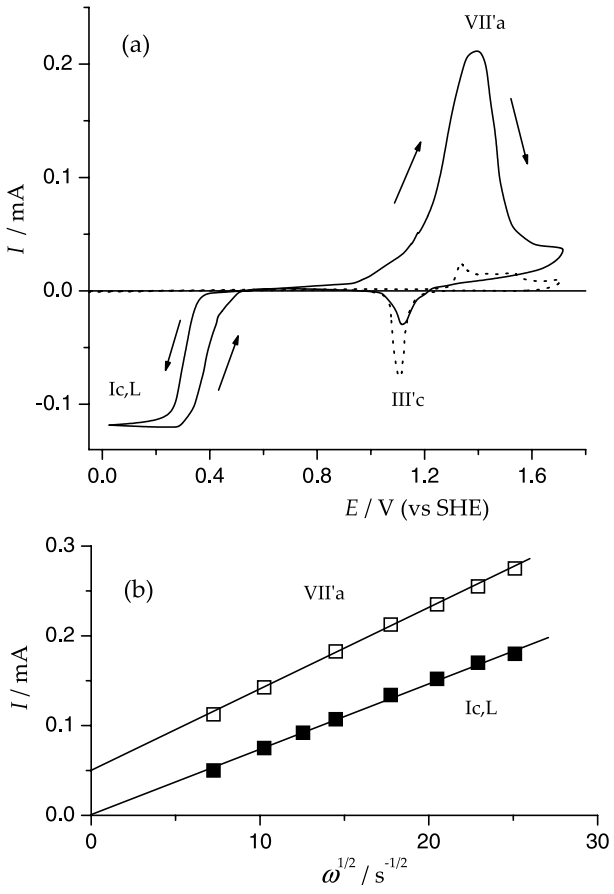

Fig. 15. (a) Cyclic voltammogram of gold in 1 mM FDS (2 mM HCl)+aqueous 0.5 M sulphuric acid at $\omega = 2000$ rpm and $v = 0.05$ V s^{-1}. (b) Dependance of peak IV′a and limiting current $I_{c,l}$ on $\omega^{1/2}$. The $I_{c,l}$ values plotted were obtained from scans run between 0.7 and 0.0 V to avoid chloride ion influence. Blank voltammogram (dotted line). $A = 0.12$ cm^2.

estimate the value of D for FDS from the slope $\Delta I_{c,l}/\Delta\omega^{1/2} = 7.39 \times 10^{-6} A$ s$^{-1/2}$; $A = 0.12$ cm^2; $n = 2$ and $v \simeq 0.01$ cm^2 s^{-1}, this results in $D_i = 4 \times 10^{-6}$ cm^2 s^{-1}, a figure that agrees reasonably well with the value 6×10^{-6} cm^2 s^{-1} that has recently been reported for FDS in aqueous sulphuric acid [19].

Peak VI′a (Fig. 15a) results from the depletion of chloride ions caused by gold electrodissolution followed by gold passivation due to the electrochemical formation of the oxygen-containing layer [23,31,32]. Consequently, the height of peak VI′a increases linearly with $\omega^{1/2}$ (Fig. 15b), the corresponding slope being $9.0 \times 10^{-6} A$ s$^{-1/2}$. This plot exhibits a positive ordinate for $\omega = 0$ that coincides with the residual current read at $E = 1.6$ V in Fig. 15. From these data, after baseline correction, the value of the diffusion coefficient of chloride ions 1.4×10^{-5} cm^2 s^{-1} as reported earlier [37], is obtained.

3.4. Electro-oxidation of adsorbates from FDS- and sulphide-containing solutions

To verify the possible contribution of sulphur/sulphide adsorption from byproducts from either TU or FDS formed either chemically or electrochemically voltammetric runs utilising sulphide-containing solutions were performed. In this case, current peak are denoted with double roman primes. Under comparable conditions, both FDS and sulphide-containing solutions produce adsorbates on gold (Fig. 16a). The voltammetric electro-oxidation of adsorbates from FDS is similar to that resulting from TU (Fig. 9a and b). Conversely, the voltammetric electro-oxidation of sulphide species from 1 mM sodium sulphide+0.5 M sulphuric acid occurs from 1.3 V upwards, showing peak III″a and a new peak VII″a related to the electro-oxidation of sulphide/sulphur surface species to sulphate [38], the latter appearing as peak VII′a for FDS-containing solutions.

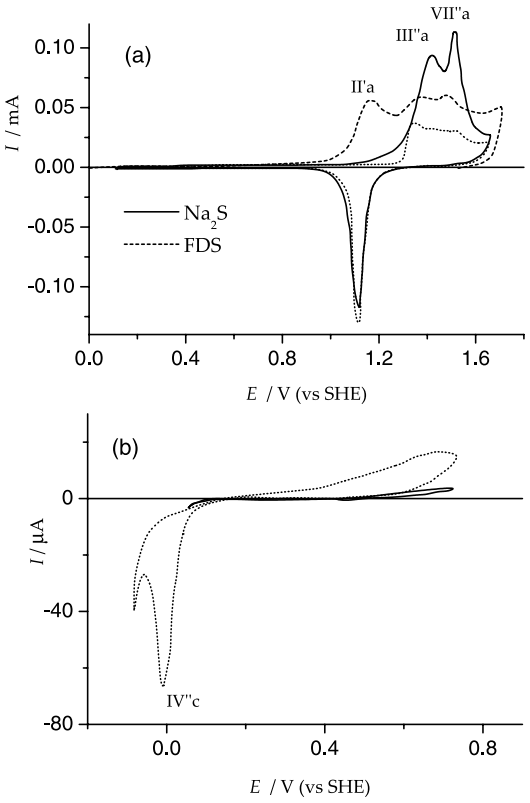

Fig. 16. Voltammograms of FDS and sulphide adsorbates electrodesorption that are formed at open circuit for 30 s. 1 mM FDS+ aqueous 0.5 sulphuic acid (dashed line); 1 mM sodium sulphide+ aqueous 0.5 M sulphuric acid (full line). (b) Cyclic voltammograms of gold in 1 mM sodium sulphide+aqueous 0.05 M sulphuric acid. $E_l = -0.08$ V, $E_u = 0.75$ V (dotted line); $E_l = 0.05$ V, $E_u = 0.75$ V (full line). $v = 0.05$ V s^{-1}.

On the other hand, runs in the range 0.1–0.6 V made for gold in 1 mM sodium sulphide+0.5 M sulphuric acid exhibit practically no current (Fig. 16b). Contrarily, for $E_l = -0.08$ V, a clear cathodic current peak IV″c is recorded, the corresponding value of q_c being close to 375 ± 20 μC cm^2. Peak IV″c corresponds to the electrodesorption of sulphur as polysulphides from gold according to [38]

$$(S_{x+1})_{ad} + 2e^- \rightarrow (S^{2-}_{x+1})_{ad} \quad (2)$$

In principle, one would expect that peaks IV″c and IVc (Fig. 7) would be related to the same adsorbed sulphur species. However, the voltammetric behaviour of peak IVc differs from that of peak IV″c as the latter exhibits no conjugated electroadsorption peak (Fig. 7, peak IVa). It should be noted that voltammetric electrodesorption of sulphur species, TU and alkanethiols from gold appears at almost the same potential range [39], a fact that is not surprising if one considers that the electrodesorption Gibbs energy is dominated by the strong sulphur–gold interaction energy [40,41].

4. Discussion

4.1. Preliminary considerations

The electrochemical kinetics of gold in TU- and FDS-containing acid solution involves a number of processes occurring in the range of potential −0.25 to 1.7 V, most of the relevant processes following mass transfer kinetics influenced by the presence of different adsorbates. At low potentials (−0.25 to 0.2 V) one can distinguish chemical adsorption and electrosorption of TU and TU derivatives leading to the formation of adsorbates acting as precursors of the following reactions. At intermediate potentials (0.2–0.9 V), gold electrodissolution/electrodeposition from soluble gold complex ions, electrochemical oxidation of TU and electroreduction of FDS are observed. Finally, at high potentials (0.9–1.7 V) products from the preceding reactions are electro-oxidised and the gradual passivation of gold, caused by residual products from electro-oxidation reactions, takes place. In this range of potential there is a competitive formation of strongly bound adsorbates from TU, FDS and water, their electro-oxidation producing higher oxidation byproducts, such as sulphate and cyanamide [42–44], as well as soluble gold complex species. It should be noted that gold electrodissolution via the formation of soluble $[Au(TU)_2]^+$ complex ions occurs in both potential regions. The soluble product can be isolated as $[Au(TU)_2]_2SO_4$ crystals that exhibit a triclinic structure with four distinct $[Au(TU)_2]^+$ ions per asymmetric unit with nearly linear S–Au–S bonding, having a conformation close to that found for chloride salt [17]. The pK value of the complex ion is 21.7 at 298 K [45], i.e. its stability is relatively high as compared to copper (pK = 15) and silver (pK = 13) TU complexes [45].

4.2. The rest potential of gold in TU-containing acid solutions

The value of E_{rest} for gold in TU-containing 0.5 M sulphuric acid lies in the potential range of the TU/FDS redox couple, and it decreases as c_{TU} is increased. The E_{rest} versus log c_{TU} plot (Fig. 1) fits a reasonable linear dependence with a slope -0.090 ± 0.01 V decade^{-1} for $c_{TU} > 1$ mM and a non-linear dependence approaching a slope -0.120 V decade^{-1} for $0.25 < c_{TU} < 1$ mM with a slight influence of oxygen gas saturation. For $c_{TU} \geqslant 1$ mM, the same relationship is obtained when the gold complex ion concentration in the solution is controlled.

The redox reaction describing the electrochemistry of gold in TU-containing acid solutions has been written as [46]

$$[Au(TU)_2]^+(aq) + e^- \rightleftharpoons Au(s) + 2TU(aq) \quad (3)$$

with $E^{0'} = 0.38 \pm 0.010$ V at 298 K [46]. However, the values of E_{rest} for gold in TU-containing acid solutions

are close to those related to the reversible redox reaction

$$\mathrm{FDS(aq)} + 2\mathrm{H^+(aq)} + 2\mathrm{e^-} \rightleftharpoons 2\mathrm{TU(aq)} \quad (4)$$

with $E^0 = 0.42$ V at 298 K on platinum [30,47–49], irrespective of pH for $0 \leqslant \mathrm{pH} \leqslant 4.3$ [47], in contrast to the prediction of reaction Eq. (4). It should be noted that for reaction Eq. (4) on platinum the exchange current density is the range $2.1 \times 10^{-6} \leqslant j_0 \leqslant 14.7 \times 10^{-6} A\ \mathrm{cm^{-2}}$, and the anodic transfer coefficient $\alpha_a \simeq 0.8$ [30,49]. These data are consistent with the intermediate kinetics of reaction Eq. (4) as concluded from data presented in Sections 3.2.1 and 3.2.3. Nevertheless, considering that there is a partial voltammetric overlapping of processes (3) and (4), explanations advanced for E_{rest} should be revised in terms of a global process involving both reactions and taking into account that, in the range of E_{rest} values the gold surface in mostly covered by TU adsorbates. In this case, the equilibrium potential of gold in TU-containing aqueous acid solutions could be related to an electrochemical reaction such as

$$[\mathrm{Au(TU)_2}]^+\mathrm{(aq)} + \mathrm{FDS(aq)} + \mathrm{H^+(aq)} + 2\mathrm{e^-} \rightleftharpoons \mathrm{Au(TU)_{ad}} + 3\mathrm{TU(aq)} \quad (5)$$

where the subscript ad stands for adsorbed species from TU.

Accordingly, the Nernst equation can be written as

$$E = E^{0'} - 2.303\left(\frac{RT}{2F}\right)\log\frac{[\mathrm{TU}]^3[\mathrm{Au(TU)_{ad}}]}{[\mathrm{FDS}][\mathrm{H^+}]^2[\mathrm{Au(TU)_2(aq)}]^+} \quad (6)$$

and the slope of the E_{rest} versus c_{TU} plot results in $-2.303(3RT/2F)$, i.e. -0.090 V decade^{-1}, which fits the experimental data for $c_{TU} \geqslant 1$ mM, as well as data reported in previous work [46,50].

Conversely, as $c_{TU} \to 0$, the formation of neither FDS nor gold complex ions would be favoured, and then the potential would be determined to a great extent by the adsorption equilibrium of TU on gold, i.e. by the ratio $\theta/(1-\theta)$, where θ refers to the degree of surface coverage of gold by adsorbates. Accordingly, the deviation of the E_{rest} versus c_{TU} plot towards positive potentials for $c_{TU} \to 0.1$ mM would be related to an equilibrium such as

$$[\mathrm{Au(TU)_2}]^+\mathrm{(aq)} + \mathrm{e^-} \rightleftharpoons \{\mathrm{Au(TU)_{ad}} + \mathrm{TU(aq)} + \mathrm{H^+(aq)} + \mathrm{e^-}\} \rightleftharpoons \mathrm{Au(s)} + 2\mathrm{TU(aq)} \quad (7)$$

the corresponding Nernst equation being

$$E = E^{0'} - 2.303\left(\frac{RT}{F}\right)\log\frac{[\mathrm{TU}]^2[\mathrm{Au(s)}]}{[\mathrm{Au(TU)_2(aq)}]^+} \quad (8)$$

Therefore, from the preceding analysis, for $0 \leqslant c_{TU} \leqslant 1$ mM the limiting slopes resulting from the E_{rest} versus $\log c_{TU}$ plots are $-\infty$ as the gold complex ions concentration approaches zero ($c_{TU} \to 0$), and $-2.303(2RT/F)$ for $[\mathrm{Au(s)}]/[\mathrm{Au(TU)_2}]^+ = \text{constant}$, the latter slope being approached in the range $0.25 \leqslant c_{TU} \leqslant 1$ mM (Fig. 1).

4.3. Electrosorption and electrodesorption of TU

According to SERS [36] and STM imaging [22] data, the adsorption of TU on gold takes place with TU in a perpendicular orientation with the sulphur atom in the coordinating position. Same results have been reported for silver [51], copper [51] and iron [52] electrodes using FTIR and Raman spectroscopic techniques. The perpendicular adsorption of TU should involve its tautomeric form [53], i.e. with the sulphur and carbon atoms singly bonded to each other producing a thiol-type molecule. Then, as usually occurs with thiols [1,54], the TU molecule spontaneously adsorbs on gold as follows

$$\mathrm{TU(aq)} + \mathrm{Au(s)} \rightarrow \mathrm{Au(TU^*)_{ad}} + \mathrm{H^+(aq)} + \mathrm{e^-} \quad (9)$$

where TU* stands for a deprotonated TU adsorbate. As far as reaction Eq. (9) is concerned, the voltammograms exhibit the pair of peaks IVa/IVc in the range -0.25 to 0 V (Fig. 7) associated with a fast electrosorption process as shown by TM voltammetry (Fig. 8). The potential range where this pair of conjugated peaks is observed correlates with the potential window in which TU adsorbates on gold have been STM imaged [22]. As the potential is shifted to $E > 0.3$ V (Fig. 3), the adsorbate can be electro-oxidised yielding soluble FDS species (peak Ia). At the same time, the packing of the adsorbed TU layer on gold can increase and eventually produce adsorbed FDS [22] when TU adsorbates react with TU molecules from the solution.

TM voltammetry data for reaction Eq. (9) over the whole range of f show peaks IVc and IVa. The charge ratio of these peaks is close to 1, with a slight difference between their peak potentials (Fig. 8a). However, the corresponding charges decrease as f is increased fitting a reasonable linear $\log C_s$ versus $\log v_m$ dependence with a slope -0.5 (Fig. 8b). This dependence, which extends to data from conventional voltammetry, indicates that the kinetics of reaction Eq. (9) are largely limited by mass transfer of TU molecules from the solution. On the other hand, the anodic and cathodic reactions might be not strictly symmetric processes, as has been observed for alkanethiol electrodesorption from gold (1 1 1) [55].

The electroreduction process is related to surface species that have been already adsorbed under open circuit conditions (Fig. 7) and mostly removed from the surface during the first negative scan from E_{rest} to -0.2 V. For $E_{ad} = E_{rest}$ and $t_{ad} = 20$ min, the charge related to peak IVc during the first negative scan (Fig. 7) is 264 $\mu\mathrm{C\,cm^{-2}}$, a figure close to the monolayer charge assuming 1 $\mathrm{e^-}$ per site per molecule. Therefore, the

fast electrochemical reaction related to peak IVc can be assigned to the electrosorption/electrodesorption of TU according to Eq. (9). This is consistent with FTIRS data reported for TU adsorption on copper in acid, which indicates that the partial desorption of TU occurs for $E < E_{rest}$ and that this desorption has a reversible character [56].

The maximum coverage of gold by TU adsorbates is reached under open circuit for $t > 900$ s. Repetitive scans between -0.2 and 0.9 V decrease the amount of adsorbed TU molecules on gold due to the formation of FDS and soluble gold-TU complex ions. Correspondingly, the charge of peak IIIc gradually decreases approaching a limiting value as the stabilised voltammogram is attained. The stripping of adsorbed TU molecules also results in inhibition of FDS formation. This effect is clearly observed when E_l is switched back to 0.05 V (Fig. 7a). Likewise, as the number of potential cycles between 0.05 and 0.9 V is increased, the concentration of adsorbed TU increases. Then, reaction Eq. (9) is no longer operative, and peaks Ia/Ic appear again. It should be noted that peak IVc is also found for 1 mM FDS + 0.5 M sulphuric acid, although its charge is significantly lower than that determined from TU. This effect is due to the low concentration of TU resulting from the electroreduction of FDS.

The comparison of preceding data to those resulting from 1 mM sodium sulphide + 0.5 M sulphuric acid (Fig. 16b) allowed us to conclude that reaction Eq. (9) represents the major contribution to peak IVc, although a minor influence of sulphur adlayer electro-reduction cannot be completely discarded considering the slow chemical decomposition of TU and FDS in aqueous solutions [57].

4.4. Likely TU/FDS and Au/Au(TU)$_2$ redox reactions

The formation of FDS from TU electro-oxidation occurring simultaneously with the electrodissolution of gold via reversed reactions Eqs. (4) and (3), respectively, agrees with the dependence of E_{rest} on c_{TU} (Fig. 1) and recent FTIRS data [21]. According to the preceding discussion, these reactions proceed with the participation of adsorbates, as concluded from their mass transfer kinetics influenced by the formation of adsorbates (Fig. 3). These complex processes resemble those that has been observed for copper electrodes [29].

The participation of TU and FDS adsorbates in the electro-oxidation of TU can be represented by the reactions

$$Au(TU^*)_{ad} + Au(s) + TU(aq) \rightarrow Au_2(FDS)_{ad} + H^+(aq) + e^- \quad (10)$$

and

$$Au(TU^*)_{ad} + TU(aq) \rightarrow Au(s) + FDS(aq) + H^+(aq) + e^- \quad (11)$$

The presence of adsorbed TU or FDS has been confirmed by STM imaging [22]. Accordingly, from reactions Eqs. (10) and (11) the following equilibrium at the interface would be established

$$Au_2(FDS)_{ad} \rightleftharpoons 2Au(s) + FDS(aq) \quad (12)$$

Reactions Eqs. (10) and (11), are responsible for the appearance of peak Ia at approximately 0.6 V (Fig. 3). These reactions behave as quasi-reversible processes, their kinetics being determined by the diffusion of TU from the bulk of the solution (Figs. 4 and 6), and strongly influenced by the presence of adsorbates. This conclusion is consistent with the relatively large (> 0.1 V) peak potential difference between peaks Ia and Ic (Fig. 3).

Mechanisms for TU electro-oxidation that have previously been proposed imply the presence of radical intermediates [4,30]. However, although the existence of free radicals has been concluded from electron spin resonance data during the homogeneous oxidation of TU by hydrogen peroxide [58], at present, there is no direct evidence of free radicals during the electrochemical oxidation of TU on metal substrates [4].

The preceding discussion can be extended to the electroformation of soluble gold complex ions. Accordingly, this reaction can be described as two consecutive electron transfer steps, the first one being the electroadsorption of TU according to reaction Eq. (9) followed by the formation of the gold–TU complex ions

$$Au(TU^*)_{ad} + TU(aq) + H^+ \rightarrow [Au(TU)_2]^+ + e^- \quad (13)$$

Considering that the electrodissolution of gold in TU-containing environments can be favoured by the presence of an oxidant in the solution [8], as FDS has been reported to be an efficient oxidant at pH < 1.7 [19], the following chemical reactions would become feasible in our system

$$Au_2(FDS)_{ad} + 2H^+(aq) + 2TU(aq) \rightleftharpoons 2[Au(TU)_2]^+(aq) \quad (14)$$

$$2Au(s) + FDS(aq) + 2TU(aq) + 2H^+(aq) \rightarrow 2[Au(TU)_2]^+(aq) \quad (15)$$

The electroreduction of both FDS and gold complexes is a competitive process (Fig. 5), its relative voltammetric charge contribution depending on v. As v is decreased, the electrodissolution of gold prevails over the formation of FDS, as results from their electroreduction charges (Fig. 5). This is in agreement with the approximately 100% gold electrodissolution efficiency that has been found under potentiostatic conditions for $E < 0.3$ V [18].

The soluble gold complex is electroreduced during the negative potential scan resulting in the appearance of peak IIc (Fig. 3). This peak increases as c_{TU} is increased from 1 to 10 mM, and disappears as E_u is decreased from 0.95 to 0.65 V (Fig. 3b and c). Peak IIc is absent in the voltammograms from FDS-containing solutions (Fig. 4). In this case, the formation of gold complex is expected to be quite low so that contribution of peak IIc is likely to be obscured by the electroreduction of FDS itself.

4.5. Further electrochemical processes for $E > 0.9$ V

From 0.9 V upwards, the voltammograms of gold in TU-containing solutions exhibit a current increase that eventually results in the appearance of two peaks, one just before the threshold potential of the oxygen-containing layer formation on gold, and another one in the potential range where a full oxide layer from the discharge of water on gold is produced (Figs. 2 and 10). The height of peaks IIa and IIIa increases linearly with ω, although the slope of these lines does not change proportionally to c_{TU}, because of the blockage of the electrode surface by adsorbates resulting from further electro-oxidation of TU and FDS. The hysteresis loop shown in Fig. 10 inset, indicates that the electrodissolution of gold (peak IIa) is hindered by the passivation of the gold surface [18], as concluded from RRDE experiments (Fig. 12). Below 1.3 V, when the electroreduction of the oxygen-containing layer on gold commences, the reactivation of the gold electrodissolution reaction takes place.

For $E > 0.9$ V, the electro-oxidation of surface species can be explained in terms of processes I and II, referred to in Section 3.2.2. Process I is related to the appearance of S- and CN-containing adsorbates either from TU via $Au(TU^*)_{ad}$

$$Au(TU^*)_{ad} + Au(s) \rightarrow Au(S)_{ad} + Au(CN)_{ad} + \tfrac{1}{2}N_2(g) + 3H^+(aq) + 3e^- \quad (16)$$

or from FDS via $Au_2(FDS)_{ad}$

$$Au_2(FDS)_{ad} + Au(s) \rightarrow Au(S)_{ad} + 2Au(CN)_{ad} + N_2(g) + 6H^+(aq) + 6e^- \quad (17)$$

On the other hand, process II is associated with the anodic formation of soluble products via the anodic stripping of adsorbates. The voltammetric electro-oxidation of TU, FDS and sulphide adsorbates (Figs. 9 and 16) indicates that at high potentials, soluble sulphate appears as a common product. Then, process II can be expressed by a reaction such as

$$Au(S)_{ad} + Au(CN)_{ad} + 6H_2O \rightarrow 2Au + SO_4^{2-}(aq) + CO_2(g) + \tfrac{1}{2}N_2(g) + 12H^+(aq) + 10e^- \quad (18)$$

It should be noted that FDS in acid solutions is rather unstable and slowly decomposes irreversibly into elemental sulphur and cyanamide [8,10], which eventually results in the formation of adsorbed residues that are electro-oxidised at $E > 1.2$ V (Fig. 9). In fact, STM imaging of gold(1 1 1) in TU-containing perchlorate solutions has shown that sulphur octomers are produced on the electrode surface at potentials above those corresponding to the electro-oxidation of TU to FDS [22].

Reaction Eq. (18) is accompanied by the simultaneous formation of the oxygen-containing layer from water electro-oxidation on gold.

$$H_2O + Au(s) \rightarrow Au(O)_{ad} + 2H^+(aq) + 2e^- \quad (19)$$

The electroreduction of this adlayer takes place for $E < 1.3$ V (peak IIIc). The kinetics and likely mechanism of this reaction have been extensively described [23,31,32].

The voltammetric charge ratio of TU adsorbate electro-oxidation (reactions Eq. (16)+Eq. (18))/electroreduction of oxygen adlayer (reaction Eq. (19), in the reverse direction) is 6.5, a figure higher than the value of approximately 3 experimentally found (Fig. 9). This difference can be explained by the formation of soluble products from TU in solution with a lower oxidation state, such as CN-containing species, as expressed by the reaction.

$$2TU(aq) + 10H_2O \rightarrow H_2NCN(aq) + 2SO_4^{2-}(aq) + CO_2(g) + N_2(g) + 26H^+(aq) + 22e^- \quad (20)$$

The presence of CN-containing species has been confirmed from FTIRS data of TU electro-oxidation on platinum [42] and more recently CN bands have been observed from FTIRS spectra related to the electro-oxidation of TU on gold in acid [21].

According to the reactions above, the complete electro-oxidation of TU on gold can be expressed by the overall reaction.

$$TU(aq) + 6H_2O \rightarrow SO_4^{2-}(aq) + CO_2(g) + N_2(g) + 16H^+(aq) + 14e^- \quad (21)$$

The products in solution (sulphate and carbon dioxide) have been recently found by in situ FTIRS [21].

5. Conclusions

(1) For $c_{TU} > 1$ mM, the equilibrium potential of gold electrodes immersed in TU-containing sulphuric acid solutions is determined by an electrochemical reaction involving adsorbed TU, FDS and soluble $[Au(TU)_2]^+$ complex species. The slope of the E_{rest} versus log c_{TU} plot is -0.090 V decade^{-1}. For $c_{TU} < 1$ mM, the slope of this plot increases approaching a value of -0.120 V decade^{-1}. This can be explained by the equilibrium involving adsorbed TU and $[Au(TU)_2]^+$ complex ions.

(2) The electrosorption process of TU on gold involves fast electron transfer reactions producing TU adsorbates under diffusion control, as concluded from TM voltammetry. Adsorbed TU species act as precursors of FDS formation and gold dissolution.

(3) The electro-oxidation of TU and the electrodissolution of gold in the presence of TU are competitive processes. Both reactions proceed under mass transport control influenced by adsorbates produced on gold.

(4) The main electro-oxidation reactions are accompanied by the formation of surface species, i.e., sulphur-, CN- and O-containining adsorbates that interfere with the kinetics of these electro-oxidation reactions.

(5) Sulphur and CN-containing surface species are electro-oxidised for $E > 1.2$ V yielding sulphate, carbon dioxide and nitrogen.

Acknowledgements

This work was supported financially by the Consejo Nacional de Investigaciones Científicas y Técnicas (CONICET), Agencia Nacional de Promoción Científica y Tecnológica of Argentina (PICT 98 06-03251) and the Comisión de Investigaciones Científicas de la Provincia de Buenos Aires (CIC).

References

[1] A. Ulman, Chem. Rev. 96 (1996) 1533.
[2] V. Brunetti, B. Blum, R.C. Salvarezza, A.J. Arvia, P.L. Schilardi, A. Cuesta, J. Gayone, G. Zampieri, J. Phys. Chem. B 106 (2002) 9831.
[3] P. Cofre, A. Bustos, J. Appl. Electrochem. 24 (1992) 564.
[4] H. Zhang, I.M. Ritchie, S.R.L. Brooy, J. Electrochem. Soc. 148 (2001) D146.
[5] B. Pesic, T. Seal, Metall. Trans. 21B (1990) 419.
[6] V. Gaspar, A.S. Mejerovich, M.A. Meretukov, J. Schmiedl, Hydrometallurgy 34 (1994) 369.
[7] L. Tremblay, G. Deschênes, E. Ghali, J. McMullen, M. Lanouette, Int. J. Miner. Process 48 (1996) 225.
[8] T. Kai, T. Hagiwara, H. Haseba, T. Takahashi, Ind. Eng. Chem. Res. 36 (1997) 2757.
[9] S. Aguayo Salinas, M.A. Encinas Romero, I. González, J. Appl. Electrochem. 28 (1998) 417.
[10] L. Chai, M. Okido, W. Wei, Hydrometallurgy 53 (1999) 255.
[11] F. Hanic, E. Durcanská, Inorg. Chim. Acta 3 (1969) 293.
[12] M.B. Ferrari, G.F. Gasparri, Cryst. Struct. 5 (1976) 935.
[13] R.C. Bott, G.A. Bowmaker, C.A. Davis, G.A. Hope, B.E. Jones, Inorg. Chem. 37 (1998) 651.
[14] O.E. Piro, R.C.V. Piatti, A.E. Bolzán, R.C. Salvarezza, A.J. Arvia, Acta Cryst. B56 (2000) 993.
[15] P.M. Henrichs, J.J. Ackerman, G.E. Maciel, J. Am. Chem. Soc. 99 (1977) 2544.
[16] L.C. Porter, J.P. Fackler, J. Costamagna, R. Schmidt, Acta Cryst. C48 (1992) 1751.
[17] O.E. Piro, E.E. Castellano, R.C.V. Piatti, A.E. Bolzán, A.J. Arvia, Acta Cryst. C58 (2002) 252.
[18] T. Groenewald, J. Appl. Electrochem. 5 (1975) 71.
[19] J. Li, J.D. Miller, Hydrometallurgy 63 (2002) 215.
[20] T. Groenewald, Hydrometallurgy 1 (1976) 277.
[21] A.E. Bolzán, T. Iwasita, A.J. Arvia, J. Electroanal. Chem., in press.
[22] O. Azzaroni, B. Blum, R.C. Salvarezza, A.J. Arvia, J. Phys. Chem. B 104 (2000) 1395.
[23] R. Woods, in: A.J. Bard (Ed.), Electroanalytical Chemistry, vol. 9, Marcel Decker, New York, 1976, p. 98 (chapter 1).
[24] B.E. Conway, H. Angerstein-Kozlowska, F.C. Ho, J. Klinger, B. MacDougall, S. Gottesfeld, Disc. Faraday Soc. 56 (1973) 210.
[25] A.E. Bolzán, A.C. Chialvo, A.J. Arvia, J. Electroanal. Chem. 179 (1984) 71.
[26] J.O. Zerbino, N.R. de Tacconi, A.J. Arvia, J. Electrochem. Soc. 125 (1978) 1266.
[27] N.R. de Tacconi, J.O. Zerbino, A. Arvia, J. Electroanal. Chem. 79 (1977) 287.
[28] A.E. Bolzán, I.B. Wakenge, R.C. Salvarezza, A.J. Arvia, J. Electroanal. Chem. 475 (1999) 181.
[29] A.E. Bolzán, I.B. Wakenge, R.C.V. Piatti, R.C. Salvarezza, A.J. Arvia, J. Electroanal. Chem. 501 (2001) 241.
[30] S.J.J. Reddy, V.N. Krishnan, J. Electroanal. Chem. 27 (1970) 473.
[31] C.M. Ferro, A.J. Calandra, A.J. Arvia, J. Electroanal. Chem. 65 (1975) 963.
[32] B.E. Conway, J. Electroanal. Chem. 524 (2000) 4.
[33] A.J. Bard, L.R. Faulkner, Electrochemical Methods, Wiley, New York, 1980.
[34] J. Kirchenerovâ, W.C. Purdy, Anal. Chim. Acta 123 (1981) 83.
[35] M. Alodan, W. Smyrl, Electrochim. Acta 44 (1998) 299.
[36] R. Holze, S. Shomaker, Electrochim. Acta 35 (1990) 613.
[37] J.H. Gallego, C.E. Castellano, A.J. Calandra, A.J. Arvia, J. Electroanal. Chem. 66 (1975) 207.
[38] X. Gao, Y. Zhan, M.J. Weaver, J. Electrochem. Soc. 8 (1992) 668.
[39] W. Paik, S. Eu, K. Lee, S. Chon, M. Kim, Langmuir 16 (2000) 10198.
[40] O. Azzaroni, M.E. Vela, G. Andreasen, R.C. Salvarezza, J. Phys. Chem. B, 106 (2002) 12267.
[41] V. Brunetti, B. Blum, R.C. Salvarezza, A.J. Arvia, in preparation.
[42] M. Yan, K. Liu, Z. Jiang, J. Electroanal. Chem. 408 (1996) 225.
[43] P.C. Gupta, Z. Anal. Chem. 196 (1963) 412.
[44] E.E. Reid, Organic Chemistry of Bivalent Sulfur, vol. 5, Chemical Publishing Co, New York, 1963.
[45] R.G. Schulze, J. Metals (1984) 62.
[46] V.P. Kazakov, A.I. Lapshin, B.I. Paschevitskii, Russ. J. Inorg. Chem. 9 (1964) 708.
[47] P.W. Preisler, L. Berger, J. Am. Chem. Soc. 69 (1947) 322.
[48] D.F. Suarez, F.A. Olson, J. Appl. Electrochem. 22 (1992) 1002.
[49] S.V. Gorbachev, A.F. Atanasyants, Y.M. Senatorov, Russ. J. Phys. Chem. 46 (1972) 1395.
[50] C.M. Juarez, A.J.B. Dutra, Anais do XVI Encontro Nacional de Tratamento de Minérios e Hidrometalurgia, Rio de Janeiro, Brasil (1995) 232.
[51] M. Fleischmann, I.R. Hill, G. Sundholm, J. Electroanal. Chem. 157 (1983) 359.
[52] J.O. Bockris, B.E. Conway, J. Phys. Chem. 28 (1968) 707.

[53] H. Hagenström, M.A. Schneeweiß, D.M. Kolb, Langmuir 15 (1999) 2435.
[54] S. Eu, W. Paik, Chem. Lett. (1998) 405.
[55] T. Kakiuchi, H. Usui, D. Hobara, M. Yamamoto, Langmuir 18 (2002) 5231.
[56] D. Papapanayiotou, R.N. Nuzzo, R.C. Alkire, J. Electrochem. Soc. 145 (1998) 3366.
[57] M. Hoffmann, J.O. Edwards, Inorg. Chem. 16 (1977) 3333.
[58] N. Motohashi, I. Mori, J. Inorg. Biochem. 26 (1986) 205.